

Flow Visualization and Density Measurement of Compressible Flows by a Laser Speckle Method

Hirahara, H.*¹, Kawahashi, M.*¹ and Murayama, A.*²

*1 Faculty of Engineering, Saitama University, Shimo-Okubo 255, Urawa, Saitama, 338-8570, Japan.

*2 Kanto Auto Works Ltd., Yokosuka, Kanagawa, 237-8585, Japan.

Received 24 September 1999.

Revised 24 September 1999.

Abstract: Laser speckle method is a well known technique that is useful for both visualization and quantitative measurement. This technique was applied to the density measurement of Mach reflection of shock waves in the present experiment. The Object of the measurement is the density field of simple Mach reflection in relatively low shock Mach number. The non-uniform flow field is divided into three regions by incident, Mach and reflected shock waves. A shock tube was employed in the present experiment. Wedges of 20 degrees and 45 degrees were placed in the test section. YAG laser was employed as a light source. Speckle photograph was taken by a digital still camera. Simple subtraction between the reference and flow images shows a shock pattern and a degree of the correlation of speckle pattern in the flow field. Thus, we can obtain a visualized flow image showing a configuration of Mach reflection from speckle photograph. Speckle photographs which was obtained in the experiments were processed with cross-correlation method. A reconstructed density gradient vector map of Mach reflection was obtained. Comparing the experimental result with numerical one, the measured density gradient shows a good agreement with theoretical prediction.

Keywords: laser speckle photography, density measurement, compressible flow, shock tube.

1. Introduction

In order to investigate a compressible flow field, well-known conventional techniques as shadowgraph, schlieren and interferometric technique are also useful for the measurement of density distribution. These are used to be applied to flow visualization in many cases. As well-known in general, these techniques would be adopted in many cases according to the respective situation. For example, shadowgraph is suitable for the visualization of flow field including a strongly varied density field, which image gives us a second derivative of density distribution in space. Schlieren image gives a first derivative of that, and also, an interferometric technique is excellent one for density measurement with high resolution. On the other hand, laser speckle method such as speckle photography, speckle interferometry, digital speckle pattern interferometry, etc. are also widely accepted for the measurement of solid displacement, flow velocity and density field in general. Especially, speckle photography has a feature that both visualization and quantitative measurement are available. Laser speckle photography gives us a first derivative of density distribution, and its information is included implicitly in the image. We can use a correlation analysis in order to reconstruct a first derivative of density distribution. Of course, speckle method includes optical speckle noises in the image inherently, nevertheless, laser speckle method is peculiar to its easiness of practical application in contrast to the other method. This method has an advantage with quantitative measurement of velocity (Merzkirch, 1987; Kawahashi et al., 1991; Kawahashi et al., 1995; Lauterborn and Vogel, 1984; Adrian, 1991) and density (Wernekinck and Merzkirch, 1987; Erbeck and Merzkirch,

1988; Koepf, 1972; Debrus, 1972), Erbeck and Merzkirch (1988) applied the speckle method to the isotropic turbulent flow, which has disturbed uniformly by heated wire in a wind tunnel. Because an interferometric method could not be applied to such a turbulent flow, the feature of speckle method was emphasized in their study. In fact, since only the light deflection is important for the density measurement in speckle photography, it is not required a long coherent light length for the laser source and then it has an advantage rather than the other optical method. The dynamic range and accuracy of measurement are variable by a simple optical arrangement regulation. Furthermore, its simple optical set-up is able to be adopted to any test field not only inside laboratory but also test field outside. This is a most impressive advantage in practical application.

In the present paper, we applied this method to the density gradient measurement of Mach reflection of shock waves as a typical phenomena in compressible flow. The phenomena of Mach reflection have been investigated by many other researches. Previous experimental results have been compared and discussed with numerical one. The configuration has been discussed for a several decades. A lot of experiments have been carried out to make the shock reflecting process clear by shadowgraph technique, schlieren technique and other optical visualization technique. Most investigations were focused on the flow field near the triple point, because its feature is significant and important to determine the reflection process over the wedge. Reflected shock wave should be formed by the interaction between a shock reflection process near the triple point and flow deflection process over the compression corner. This interpretation has a meaning when discussing the weak shock reflection. In the studies on the wave propagation of shock wave or finite amplitude wave, the gradient of pressure or density near wave front is very important factor. We will apply the speckle photography for the simple Mach reflection in low shock Mach number. The flow field is not turbulent, but the flow field is divided into three regions by the incident shock wave, Mach shock wave and reflected shock wave. The density varies inside region bounded by the reflected shock wave Mach shock wave, and wedge wall. Its gradient might play an important role to determine a reflected shock configuration and triple point, especially in lower shock Mach number. Laser speckle measurement would give a distribution of density gradient directly. Speckle photographs which was obtained in the experiments were processed with a cross-correlation method in a suitable way. Experimental density gradient vector maps were compared with numerical results and examined on its accuracy.

2. Experiment

2.1 Shock Tube

Figure 1 shows a shock tube that was used in the present experiment. Two wedges of 20 degrees or 45 degrees were prepared for the experiment. N_2 gas was used as a test gas. The cross area in the test section is 80×80 mm and observation window is also 80×80 mm. Although the initial pressure in test section may be much lower than the atmospheric pressure in usual shock tube experiments, the present initial pressure in test section is fixed at 500 and 550 Torr. It is required to increase the deflection angle in order to carry out a capable measurement in moderate density. Shock speed was measured with two pressure transducers that are mounted on the side-wall just upstream of test section. Incident shock Mach number, M_s could be varied from 1 to 3 under the initial pressure. We have carried out the experiment in $M_s=1.2, 1.4$ and 1.6 .

2.2 Optical Setup and Analysis

Figure 2 shows the optical set up for the speckle photographic measurement. YAG laser (SpectraPhysics, GCR-130) was employed in the experiment. The wavelength of the laser is 532 nm, the maximum output 200 mJ/pulse and pulse duration 7 ns. The test section (the centerline of shock tube), an achromatic lens ($\phi 100$ mm, $f=375$ mm) and a ground glass were placed 750 mm apart from each other. Therefore, the image of test section is focused on the ground glass. On the ground glass, a speckle pattern would be produced. Camera image is defocused by l mm apart from the focused plane (ground glass). Speckle photograph was taken by a digital still camera (FUJIX, 550A, 1.3 Mpixels, ASA3200). 550A has a CCD sensor with RGB masked filter. The obtained photograph is 1280×1080 pixels RGB raw data and 8 bit resolution. The RGB raw data was decomposed in R, G, and B plane. Then, a green plane only was used for analysis. In this manner, the photo image was converted to monochrome image of 8 bit. Speckle size on the camera image plane is determined by F-number of lens and aperture size. The speckle size was adjusted with an aperture in front of camera lens. The effective image size is 800×800 pixels. The test field was projected to 800×800 pixels area. Since the observation window area is 80×80 mm, the space resolution of the present measurement is 0.1 mm/pixels. The procedure of recovery for density gradient by a

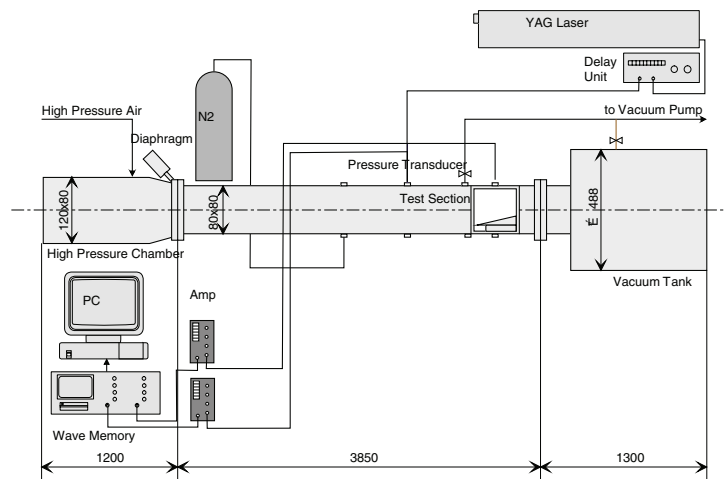


Fig. 1. Schematic of shock tube.

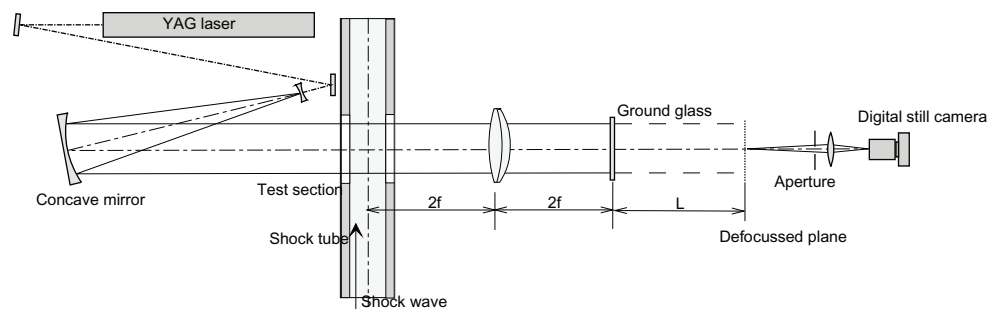


Fig. 2. Optical setup of speckle photography.

correlation analysis will be described in the succeeding section.

Fundamental relation between the density gradient and speckle displacement is well known and very simple one. Object beam passing through the test section might be deflected by the angle $(\varepsilon_x, \varepsilon_y)$ where x, y is the coordinates in a plane parallel to the shock propagating direction. $(\varepsilon_x, \varepsilon_y)$ is related to the density gradient for the respective direction with the following equation.

$$\varepsilon_i = K \int \frac{\partial \rho}{\partial i} dL, \quad i = x, y \quad (1)$$

K is the Gladstone-Dale constant, ρ the fluid density, L the width along the optical path of the test section. ε_x and ε_y are calculated by the correlation function for the obtained speckle pattern. The reference images were taken before the respective test runs. $(\varepsilon_x, \varepsilon_y)$ are calculated with the displacement of speckle pattern from the reference and flow images. Then, a simple relation, $\varepsilon_i = \delta_i / l$ gives a deflection angle of speckle over the image plane, where δ_i is speckle displacement in the recorded plane. We applied the cross-correlation analysis for the calculation of the speckle displacement. Cross-correlation analysis is based on the residual accumulation of intensity difference. A fast algorithm described in the report by Kaga et al. (1991) was adopted to obtain a deflection angle as a cross-correlation method, which is a sort of pattern tracking method. This algorithm is simple and able to obtain a correlation in very short time. The sizes of the interrogation, 8×8 , 16×16 and 32×32 pixels were examined in the analysis. Following the above method, the maximum correlation point is determined as a point where the amount of the residue of intensity difference between the two interrogation regions becomes minimum. Of course, the smaller the interrogation size was selected, the larger the error of correlation became. The most reasonable vector map was obtained in 16×16 pixels interrogation size. The error vector increased in 8×8 pixels interrogation although at least 1×10^4 vectors should be obtained with this interrogation size. On the other hand, enough resolution was not obtained in 32×32 pixels although the minimum error vectors were obtained in the present analysis. In general, sub pixel analysis is sometimes used in order to improve the space resolution in such as PIV

measurement. Also, in the present analysis, sub-pixel speckle displacement was detected by a curve fitting of two-dimensional parabolic function, $f=ax^2+by^2+cxy$ for the correlation plane, in which an algorithm of least square method was used. The accuracy of the measurement depends on that of speckle displacement, δ_i . If the accuracy of δ_i is held in sub-pixels, the accuracy of this measurement should be kept in two or three digits at least. It may not be high accuracy, however, the dynamic range of the measurement can be varied in a wide range by choosing a suitable defocus length l . This is the most advantage of this measurement.

3. Numerical Prediction

Numerical simulation was carried out by a finite difference method. We solved the unsteady Mach reflection phenomena with TVD scheme. The present scheme is first order in time and third order in space. Computational grid is constructed with oblique lattices of 600×400 mesh size. TVD scheme is examined enough by many researchers, then its validity for high speed flow with shock wave was confirmed in the previous experiments except in the case of weak Mach reflection. When a weak shock wave reflect over the wedge, it should be still discussed in detail in the future. In the present study, the calculation was carried out with CFL number 0.1. Non-slip boundary condition was constrained on the wedge surface.

Numerically predicted density maps and vector maps of density gradient were demonstrated in Figs. 3 and 4. Figures 3(a) and 4(a) are density maps of Mach reflection. Under the present condition, Mach reflection only is possible for the given shock Mach number and wedge angle. As shown in these figures, when a wedge angle is 20 degrees, the density at the corner is larger than that at triple point. Conversely, when a wedge angle is 45 degrees, the density at the triple point is much larger than that at the corner. In this case, a large density gradient is formed near the triple point. There are two maximum density peaks in the field, then the density vectors should be converging upon the wedge apex and the triple point.

In Figs. 3(b) and 4(b), density gradient is shown in vector form. The density gradient was calculated in non-dimensional form, so the vector size was demagnified by a factor 0.05 for convenience. This treatment is conformed with the dimensional reduction of experimental data processing described in Section 4.2. These vector maps were superimposed on the density colour contour map. Shock front is presented with 4 or 5 grids width. So, the density gradient vectors inside numerical shock layer are not illustrated in these figures. The magnitude of the vector is large near the reflected shock front, the triple point and the corner. When a wedge angle is small, the slip stream is emerged from the triple point. The slipstream is a discontinuity of density and temperature. The density in the upside region of slipstream is higher than that in the downside region. The density ratio across the slipstream is about 1.1 to 1.3 in the present condition.

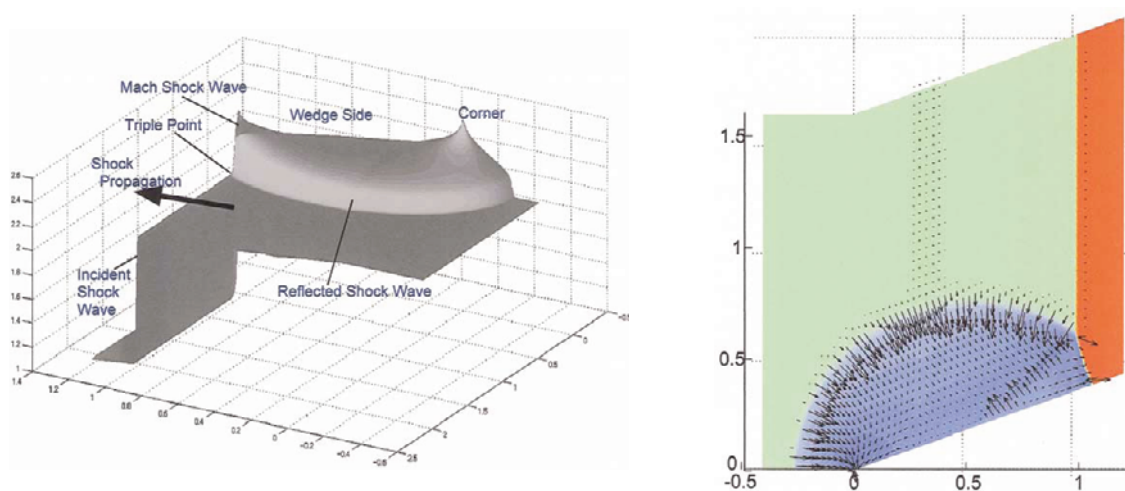


Fig. 3. Numerical prediction, $Ms=1.6$, $\theta=20$ degrees: (a) density distribution; (b) density gradient vector map.

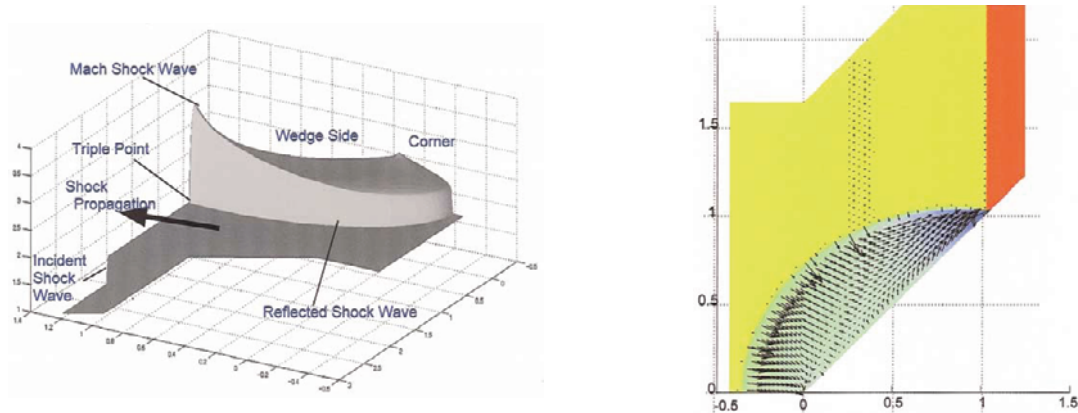


Fig. 4. Numerical prediction, $Ms=1.6$, $\theta=45$ degrees: (a) density distribution; (b) density gradient vector map.

4. Results and Discussion

4.1 Intensity Difference between Images

Figures 5(a) and (b) show the speckle patterns of the reference and Mach reflection of shock waves, which were obtained in the present experiment, respectively. These images are 800×800 pixels in size. Speckle pattern in these images is random function in space. Subtracting between these images, however, we can obtain the intensity difference, which indicates the modulation of the speckle pattern. Moderate speckle size, 3 to 5 pixels, was chosen for the measurement in the present experiment. The subtracted image gives us the effective area in the measurement and shock pattern simultaneously. Figure 6 shows the result of the subtraction. In this figure, a shock pattern was made visible which was extracted from Fig. 4(b). This simple image has been limited in quantitative meaning, but is useful for the flow visualisation and to check the measurement accuracy in space resolution. As shown in this figure, shock reflected pattern is clearly extracted from speckle photograph. Here, the incident shock wave and Mach shock wave are strong, while the reflected shock wave is weak. Speckle pattern was modulated by these three shock waves strongly, however good correlation was not obtained for the incident and Mach shock wave as shown in the following figure, since the speckle pattern was deformed significantly by the deflected light in a very narrow region. High reliability of the measurement has been kept in the bounded region by the reflected and Mach shock waves. These results will be discussed in the next section. The subtracted image will be superimposed in the density gradient vector map.

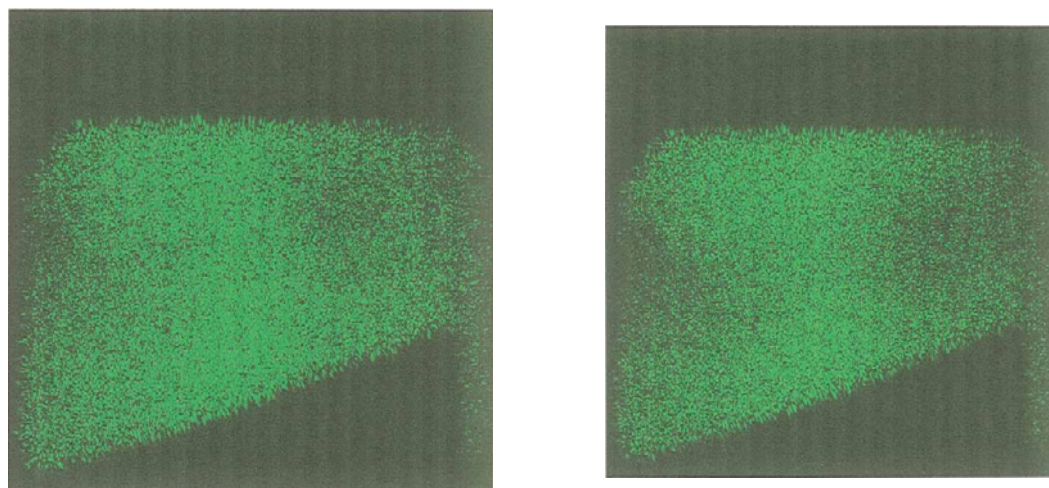


Fig. 5. Speckle images of flow field over the wedge, $\theta=20$ degrees. (a) Reference (b) Mach reflection.

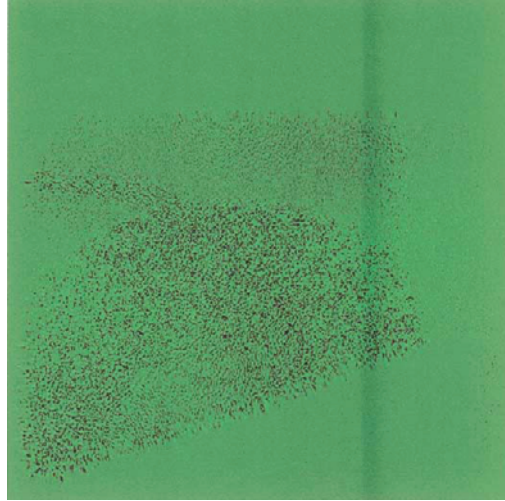


Fig. 6. Subtracted image between Fig. 5(a) and Fig. 5(b), which shows Mach reflection.

4.2 Density Gradient Vector Map

Vector's components of density gradient were determined with δx and δy , which procedure was described above, at any instance from obtained speckle photograph. Since a shock configuration is self-similar in time, the density distribution expands around the apex of wedge as a centre. Therefore, the value of density gradient at any point in flow field should decrease with time. According to this reason, we have to discuss the density gradient in non-dimensional co-ordinates, $x'-y'$. Where, $x'=x/Ust$ and $y'=y/Ust$, Us is the incident shock speed. For the convenience, we introduce a non-dimensional density gradient defined as

$$\frac{\partial \rho'}{\partial x'} = \frac{\partial \rho Ust}{\partial x \rho_0}, \quad \frac{\partial \rho'}{\partial y'} = \frac{\partial \rho Ust}{\partial y \rho_0} \quad (2)$$

where, $\rho'=\rho/\rho_0$, is normalized density and ρ_0 is the initial density. Using this form for the experimental and numerical results, we will be able to discuss the validity of the measurement in general form.

Figure 7 shows the experimental density gradient for $Ms=1.2, 1.4$, and 1.6 . Initial pressure is 550, 500 and 500 Torr when $Ms=1.2, 1.4$ and 1.6 , respectively. Corresponding initial density is 0.933, 0.848 and 0.848 kg/m^3 . Interrogation size of these results was 16×16 pixels and it was shifted by 8 pixels step. Approximately, 1200 vectors were obtained for each experimental run. Effective vectors were obtained inside region bounded by reflected shock and Mach shock. Along the incident shock wave and Mach shock wave, where the density is discontinuous, effective data were not obtained from the correlation analysis. Deflected light by shock wave resulted in a low correlation near the shock wave. These obstructive factors might be removed by introducing a spatial filtering technique in the optical set-up. Obtained vectors show a good agreement with numerical results in Fig. 3(b) and Fig. 4(b). Vector patterns are similar between the two. Density vectors are converging upon the wedge apex and triple point. When a wedge angle is 20 degrees (Figs. 7(a)-(c)), a density gradient across the slipstream was also measured. The magnitude is almost valid from numerical prediction. In the region which is bounded by Mach shock wave and slipstream, the density is not uniform. There is a density gradient towards Mach shock wave. This fact is also true as shown in numerical results in Fig. 3(b). This non-uniformity is important for the consideration on the strength of Mach stem, triple point trajectory and the formation through a shock wave propagation. In Fig. 7, vectors were observed along the wedge wall. It might be caused by the effect of boundary layer. In such small area, it is very difficult to recognize the influence of boundary layer. Nevertheless, since the density gradient vectors are recovered by the correlation between the reference and flow states, we can eliminate the influence of light deflection by the wedge wall. Then, there is a possibility to measure the density distribution close to the boundary wall by using a refined optical arrangement.

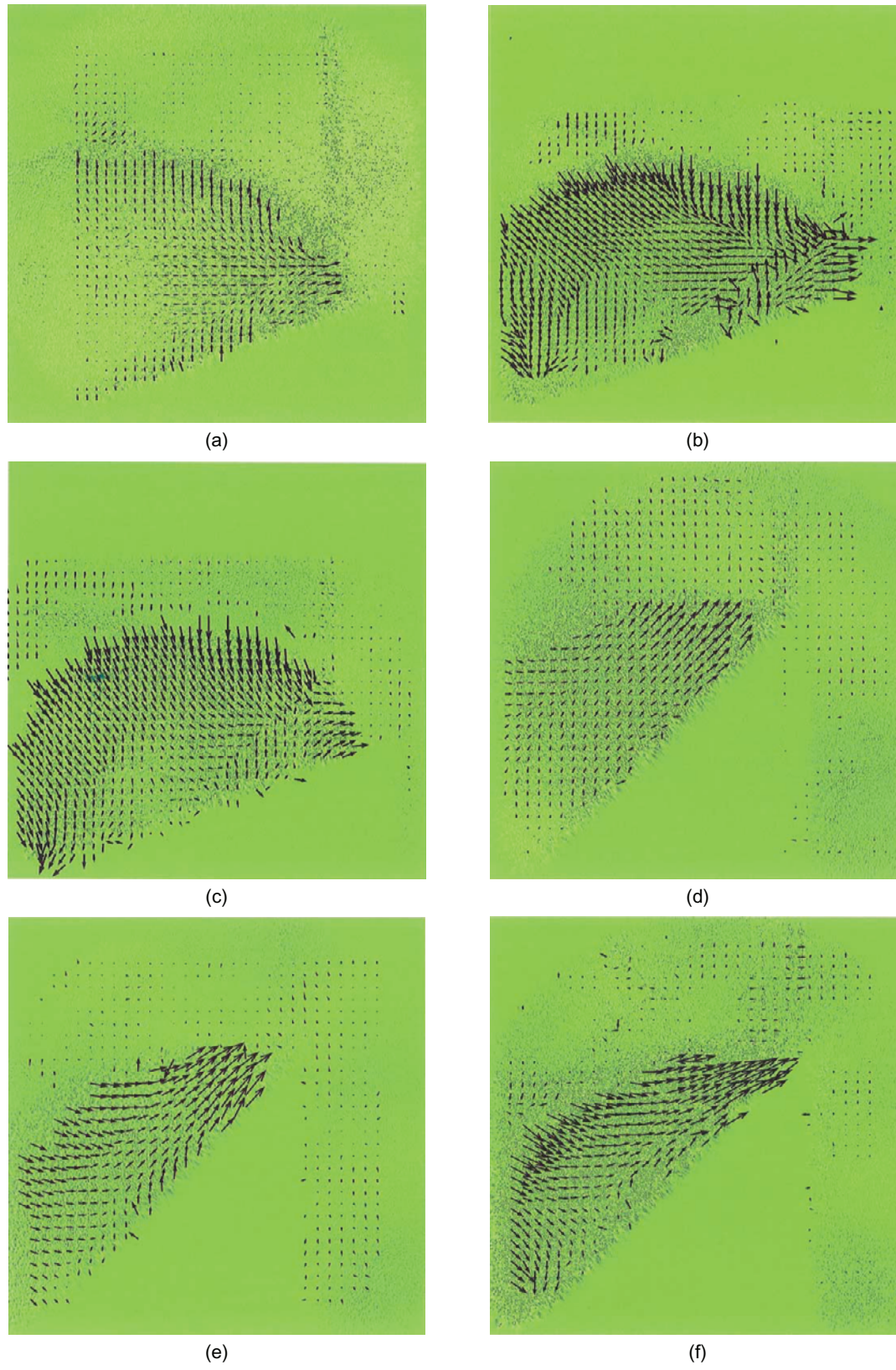


Fig. 7. Density gradient vector map obtained by the experiment:
(a) $Ms=1.2$, $\theta=20$ degrees ; (b) $Ms=1.4$, $\theta=20$ degrees ; (c) $Ms=1.6$, $\theta=20$ degrees;

5. Concluding Remarks

Density field of Mach reflection of shock waves was investigated by laser speckle photography. Density gradient was analysed and reconstructed with a correlation method from speckle photographs. Normalized density gradient, which was obtained experimentally, was compared with numerical one. Experimental density gradients were well recovered in the region bounded by a reflected shock wave, Mach shock wave and wedge wall. A good reconstructed gradient was not attained near the region where the density changed discontinuously, because the noise was included in the speckle pattern due to the deflected light.

References

- Adrian, R. J., Particle-Imaging Techniques for Experimental Fluid Mechanics, *Ann. Rev. Fluid Mech.*, (1991), 261-304.
 Debrus, S. et al., Groundglass Differential Interferometer, *Appl. Opt.*, 11 (1972), 853-857.
 Erbeck, R. and Merzkirch, W., Speckle photographic measurement of turbulence in an air stream with fluctuating temperature, *Exp. in Fluid*, 6, (1988), 89-93.
 Kaga, A. et al., Application of a Fast Algorithm for Pattern Tracking on Airflow Measurements, *Flow Visualisation VI, Proc. Sixth Int. Symp. on Flow Visualisation, Yokohama*, (1992), 853-857.
 Kawahashi, M. et al., Velocity Measurements of flows in a T-shaped Junction by Means of Dual-Beam-Sweep Laser Speckle Velocimetry, *ASME Paper, FED Vol.106, Measuring and Mating of Unsteady Flows*, (1991), 15-20.
 Kawahashi, M. et al., Speckle Method using Beam Scanning Techniques, *Proceedings of the International Workshop on PIV*, (1995), 155-158.
 Koepf, U., Application of Speckling for Measuring the Deflection of Laser Light by Phase Objects, *Opt. Comm.*, 5 (1972), 347-350.
 Lauterborn, W. and Vogel, A., *Modern Optical Technique in Fluid Mechanics*, *Ann. Rev. Fluid Mech.*, (1984), 223-244.
 Merzkirch, W., *Flow Visualization*, (1987), 60, Academic Press.
 Wernekinck, U. and Merzkirch, W., Speckle Photography of Spatially extended Refractive-Index Fields, *Applied Optics*, 26-1 (1987), 31-32.

Author Profile



Hiroyuki Hirahara: He received his Master of Mechanical Engineering degree in 1983, and his Doctor of Engineering degree in 1986 in Kyushu University. After the DE course, he worked in atomic power plant engineering section in Toshiba Co. Ltd. He worked as a Research Assistant and a Lecturer of Saitama University, before taking up his current position. He is an Associate Professor of Saitama University, and his research subjects are high speed flow, supersonic flow with condensation or evaporation, flow measuring techniques, optical measurement techniques and environmental fluid mechanics.



Masaaki Kawahashi: He received his MSc(Eng) degree in mechanical engineering in 1968 from University of Electro-Communication, and his D.Eng. in 1978 from the University of Tokyo. After MSc he worked as a Research Assistant, a Lecturer, and an Associate Professor at Saitama University before taking up his current position as a Professor at Saitama University. His research interests in thermo-fluid phenomena induced by finite amplitude wave motion in ducts, speckle metrology, and PIV measurement of complicated flow field like in centrifugal fan.



Atsushi Murayama: He received his master degree in mechanical engineering from Saitama University. He works at Kanto Auto Works Ltd.